## Introduction

Bcl11b/Ctip2 belongs to the family of zinc-finger transcription factors and is expressed in various cell types in many different tissues, such as T cells, neuronal cells, ameloblasts in teeth and certain cell types in the skin [1, 9, 10, 31]. Although *Bcl11b* knockout mice die soon after birth, newborn mice show differentiation arrests of αβ T cells in the thymus [31], malfunction of motor neurons [1], developmental tooth defect [10], and impairment of epidermal development [9]. On the other hand, $Bcl11b^{+/-}$ heterozygous mice appear normal but are susceptible to thymic lymphomas when they are subjected to gamma radiation [15]. In *in vitro* studies, selective inhibition of Bcl11b in Jurkat cells leads to cell cycle arrest and apoptosis [12, 16]. These data suggest that Bcl11b is involved in differentiation, cell proliferation and survival in different cell types. However, it is not known how Bcl11b contributes to these phenotypes, though several target genes of *Bcl11b* have been demonstrated. These genes include cell cycle inhibitors, $p21^{Cip1}$, $p27^{Kip1}$ and $p57^{kip2}$ [4, 16, 28], and a transcription factor, Msx2 [10].

Presbycusis or age-related hearing loss (AHL) is one of the most common chronic health problems of elderly individuals and adversely affects the quality of their lives. About a half of the population are affected by the age of 80 [11, 20, 21]. Presbycusis is multifactorial, combining genetic predispositions and the aging process with a plethora of lifetime insults to the auditory organ. One of the etiological classes of presbycusis is the sensory type that exhibits hair cell loss with subsequent neural degeneration [21, 24]. AHL accompanying hair cell loss is also found in mouse models of AHL. The C57BL/6(B6) strain is one such model, exhibiting degeneration of hair cells with potentially complete loss of hair cells by one year of age [24]. Hence, this model is used for the analysis of loss of hearing sensitivity and concomitant impairment of cells in the cochlea [18, 27].

In a preliminary examination, we detected Bcl11b expression in cells of the mouse cochlea. This prompted us to test whether or not impaired expression of Bcl11b is associated with AHL. Here we describe Bcl11b expression in outer hair cells, and AHL and morphological changes in the cochlea of *Bcl11b*$^{+/-}$ heterozygous mice.

## Materials and Methods

### *Animals*

*Bcl11b*$^{+/-}$ mice of the BALB/c background were bred as described previously [1, 5]. Backcrossing them to B6 mice for more than seven generations produced *Bcl11b*$^{+/-}$ mice with a B6 background. Mice used in this study were maintained under specific pathogen-free conditions in the animal colony of Niigata University. Genotyping of the mice was carried out by polymerase chain reaction as described previously [31].

### *Auditory brainstem response analysis*

Analysis of the auditory brainstem response (ABR) was performed to examine hearing activity as described previously [22]. In anesthetized mice placed in a closed acoustic room, stainless-steel electrode was inserted subcutaneously into the vertex (positive pole), retroauricular region (negative pole), and opposite retroauricular region (background) of each mouse. Individual hearing loss was quantified based upon the threshold shift between pre- and post-exposure ABR thresholds. As for noise-induced hearing loss, ABR thresholds were measured in mice at 2 months of age, as described previously [19]. The cage was positioned under a speaker so that the sound pressure within the cage varied by less than 2 dB sound

pressure level (SPL) at 100 dB. The noise was a pure tone of 10 kHz frequency, the SPL was 100 dB, and the duration was for 1 h. The noise was calibrated before each exposure session.

*Morphological analyses*

Conventional histology, immunohistochemistry and scanning electron microscopy examinations were performed, as described previously [22, 31]. Six-month old mice were anesthetized and perfused with 2% paraformaldehyde and 2% glutaraldehyde in 0.15 M cacodylate. Cochleae were dissected, fixed in 4% paraformaldehyde overnight, and then decalcified in 5% EDTA/PBS for 2 weeks. The tissues or fixed newborn cochlear tissues were dehydrated, embedded in paraffin, sectioned (4 μm), and stained with hematoxylin and eosin or antibodies (rat anti-Bcl11b/Ctip2 antibody (1:100, abcam ab18465). After washes with PBS, the sections were incubated with a secondary antibody, rat N-histofine-R Simple Stain MAX PO (Nichirei), for 1 h, then washed 3 times in PBS. Bcl11b was visualized by development with DAB in 0.05 M TrisHCl (pH 7.6) with 0.02% v/v $H_2O_2$ for 30 min. The sections were counterstained with hematoxylin. For scanning electron microscopy, mice were fixed through the heart with a buffer containing 0.9% saline, 2% glutaraldehyde and 0.1 M phosphate (pH 7.4). Immediately after perfusion, the cochleae were removed and immersed in the same fixative for more than four days at 4 °C. After decalcification for 4 h, they were treated with 1% tannic acid solution for 3 h, washed in distilled water for 1 h, and immersed in 1% $OsO_4$ solution for 4 h at room temperature. The specimens were then dehydrated in a graded ethanol series, transferred to isoamyl-acetate, and critical point-dried using liquid $CO_2$. The dried specimens were coated with platinum-palladium in an ion coater and examined on a Hitachi S2380N scanning electron microscopy at an acceleration voltage of 10 kV.

*Statistical analysis*

The unpaired t-test was used for statistical analysis. Differences were considered to be statistically significant when the P value was less than 0.05.

**Results**

*Bcl11b expression*

We obtained *Bcl11b*$^{-/-}$ and *Bcl11b*$^{+/+}$ newborn mice by crossing *Bcl11b*$^{+/-}$ heterozygous mice and immunohistochemically examined Bcl11b expression in cells of the cochlea (Fig. 1A). The organ of Corti resides on the basilar membrane and typically comprises one row of inner hair cells and three rows of outer hair cells interdigitated with several types of morphologically distinct non-sensory supporting cells. Analysis of *Bcl11b*$^{+/+}$ mice revealed Bcl11b expression in the outer hair cells but not in the inner hair cells. No expression was detected in other cell types in the cochlea including spiral ganglion cells. In contrast, *Bcl11b*$^{-/-}$ mice did not show Bcl11b expression in the outer hair cells. Despite *Bcl11b*$^{-/-}$ mice lacking the Bcl11b expression, they did not show any marked change in the morphology of the cochlea. One exception to this was the impaired formation of stereocilia at the top of outer, but not inner, hair cells in *Bcl11b*$^{-/-}$ mice, as revealed by scanning electron microscopy (Fig. 1B).

*Hearing function in heterozygous Bcl11b*$^{+/-}$ *mice*

Outer hair cells are assumed to be the mechanical amplifiers for sound sensitivity and frequency selectivity, and inner hair cells are assumed to be passive detectors of the amplified

vibratory signal [5]. We thus tested whether or not heterozygous deletion of *Bcl11b* affects hearing function by analyzing ABR, which is the evoked potential response of auditory activity in the auditory nerve and subsequent fiber tracts and nuclei within the auditory brainstem pathways. Thresholds and amplitudes of ABRs provide information on the peripheral hearing status and the integrity of brainstem pathways [13]. ABRs to frequency-specific stimulation (f-ABR) were measured in $Bcl11b^{+/-}$ and $Bcl11b^{+/+}$ mice (n=11) of B6 background over various frequency ranges at different months of age (Fig. 2A). Almost all wild-type B6 mice retained low ABR thresholds until 4 months of age; however, mice at 5 or 6 months of age showed some threshold elevations, consistent with previous studies [14, 32]. This progressive AHL in B6 mice is mainly due to their bearing the $Cdh23^{ahl}$ and *Ahl3* susceptible alleles on the chromosomes 10 and 17, respectively [14, 22, 23]. Most $Bcl11b^{+/-}$ mice showed significant increases in ABR thresholds relative to $Bcl11b^{+/+}$ mice at all ages though some still retained low thresholds. The average increases were 10-30 dB SPL at various frequencies ranging from 8 to 32 kHz (Fig. 2(A)). The hearing loss was detected in mice as early as 3 months of age at 16 and 20 kHz (P=0.038 and P=0.004, respectively). Another independent experiment showed similar results (data not shown).

We also examined BALB/c mice (n=5) that are classified as a normal hearing strain for AHL, despite carrying the $Cdh23^{ahl}$ susceptible allele [23]. Fig. 2B shows ABR thresholds at various frequency ranges in 9-month old mice. Low ABR thresholds were retained in $Bcl11b^{+/+}$ mice whereas a small increase of the ABR threshold was observed in $Bcl11b^{+/-}$ mice at 20 kHz but it was not marked at the other frequencies examined. This suggests that the effect of *Bcl11b* heterozygous deletion is small in BALB/c mice.

*Inner ear pathology in heterozygous $Bcl11b^{+/-}$ mice*

To address whether or not the observed hearing loss in *Bcl11b*$^{-/-}$ mice was accompanied by morphological alterations, we examined the hair cells of the cochlea in 6-month old *Bcl11b*$^{+/-}$ mice with AHL by scanning electron microscopy. Loss of outer hair cells in the cochlea and impairment of stereocilia were evident in some of the mice (Fig. 3A). Such abnormalities were not detected in *Bcl11b*$^{+/+}$ mice. The number of spiral ganglion cells in the cochlea of *Bcl11b*$^{+/-}$ mice seemed to differ from those of their wild-type littermates though the difference was not marked (Fig. 3B). Minimal differences were also observed in the stria vascularis of the cochlea (data not shown).

*No difference in hearing loss after acoustic trauma*

Our previous study showed that the inhibition of Bcl11b in Jurkat cells and thymocytes *in vitro* increased apoptosis sensitivity to stimulation of cell proliferation by increasing the serum concentration and DNA damage by UV irradiation [16]. This suggests that Bcl11b activity may be required for cell survival under pathological conditions. We thus examined changes in the ABR thresholds of 2-month-old B6 and BALB/c mice after noise exposure at 100 dB SPL for 60 min. Both strains exhibited significant threshold increases to 50-60 dB SPL one day after noise exposure (Fig. 4). In B6 mice this threshold shift was mostly retained at 7 and 14 days after noise exposure, and the shifts on different days did not differ between *Bcl11b*$^{+/-}$ and *Bcl11b*$^{+/+}$ mice (Fig. 4A). Also, no difference between the *Bcl11b*$^{+/-}$ and *Bcl11b*$^{+/+}$ genotypes was observed in the threshold shift in BALB/c mice, though both had restored low ABR thresholds at 14 days after noise exposure (Fig. 4B). These results suggest that the heterozygous deletion of *Bcl11b* does not affect cochlear vulnerability to noise-induced hearing loss.

**Discussion**

The results of this study show that Bcl11b transcription factor is expressed in the cell nucleus of outer hair cells, but not inner hair cells, of the mouse cochlea and that the heterozygous deletion of *Bcl11b* leads to a progressive age-related hearing loss, which was evident in mice as young as 3 months of age. Loss of outer hair cells was observed in the *Bcl11b*$^{+/-}$ mice with hearing loss at 6 months after birth. These results suggest that the AHL observed in *Bcl11b*$^{+/-}$ mice is the result of impairment of the outer hair cells, classified as the sensory type of presbycusis, and that Bcl11b activity is required for the maintenance of outer hair cells and normal hearing. However, many questions remain. For instance, how does Bcl11b protect outer hair cells and hearing function against aging? A target of Bcl11b transcription factor is *p27* [16] and *p27*$^{-/-}$ mice exhibit hearing loss [17]. However, p27 was not expressed in the outer hair cells though it was expressed in nearby supporting cells (data not shown).

The effect of the *Bcl11b* heterozygous deletion on AHL was less in BALB/c mice than B6 mice, reflecting their different genetic backgrounds. This suggests the involvement of one or more genetic loci responsible for AHL susceptibility other than the *Bcl11b* locus, though the relevant genetic difference between the two mouse strains is unknown. B6 mice carry at least two alleles (*Cdh23*$^{ahl}$ and *Ahl3*) that promote AHL and sensory hair cell loss whereas BALB/c mice are only known to carry the *Cdh23*$^{ahl}$ allele [14, 22, 23]. *Cdh23* encodes cadherin 23, a component of the tip links joining adjacent stereocilia at the top of sensory outer and inner hair cells [25, 26]. Its null mutation causes congenital deafness in mice and humans accompanying degeneration of the stereocilia of outer and inner hair cells [2, 3, 7, 30]. *Bcl11b* and *Cdh23* are both expressed in outer hair cells and affect AHL but their relationship with the development of AHL is unclear.

Mechanical stress is a factor affecting AHL, and genetic variation affects the range of individual susceptibility to mechanically induced acoustic trauma [6]. In fact, the *Cdh23*$^{ahl}$ susceptible allele renders mice more susceptible to noise-induced hearing loss than strains that do not carry this allele [8, 29]. We tested the effect of *Bcl11b* heterozygosity on cochlear vulnerability to acoustic energy exposures in B6 and BALB/c mice. However, no difference was detected between *Bcl11b*$^{+/+}$ and *Bcl11b*$^{+/-}$ genotypes in either mouse strain. This suggests that *Bcl11b* heterozygous deletion or probably the AHL-susceptible *Bcl11b*$^{+/-}$ outer hair cells do not contribute to the vulnerability to acoustic energy exposures. Hence, involvement of *Cdh23* and *Bcl11b* is different in noise-induced hearing loss.

In conclusion, *Bcl11b* heterozygosity leads to a progressive age-related hearing loss in mice. Though details of *BCL11B* mutations and polymorphisms in humans are not known, this locus may possibly affect presbycusis in humans.

**Acknowledgement**

We thank Prof. You-ichi Ajioka for performing histological examination. This work was supported by a Grant-in-aid for Transdisciplinary Research from Niigata University.

References

1. Arlotta, P., Molyneaux, B.J., Chen, J., Inoue, J., Kominami, R., and Macklis, J.D. 2005. Neuronal subtype-specific genes that control corticospinal motor neuron development in vivo. *Neuron* 45: 207–221.

2. Astuto, L.M., Bork, J.M., Weston, M.D., Askew, J.W., Fields, R.R., Orten, D.J., Ohliger, S.J., Riazuddin, S., Morell, R.J., Khan, S., Riazuddin, S., Kremer, H. , van Hauwe, P., Moller, C.G., Cremers, C.W., Ayuso, C., Heckenlively, J.R., Rohrschneider, K., Spandau, U., Greenberg, J., Ramesar, R., Reardon, W., Bitoun, P., Millan, J., Legge, R. , Friedman, T.B., and Kimberling, W.J. 2002. CDH23 mutation and phenotype heterogeneity: a profile of 107 diverse families with Usher syndrome and nonsyndromic deafness. *Am. J. Hum. Genet.* 71: 262–275.

3. Bolz, H., von Brederlow, B., Ramirez, A., Bryda, E.C., Kutsche, K., Nothwang, H.G., Seeliger, M., del C-Salcedo, M., Cabrera, M., Vila, M.C., Molina, O.P., Gal, A., and Kubisch, C. 2001. Mutation of CDH23, encoding a new member of the cadherin gene family, causes Usher syndrome type 1D. *Nat. Genet.* 27: 108-112.

4. Cherrier, T., Suzanne, S., Redel, L., Calao, M., Marban, C., Samah, B., Mukerjee, R., Schwartz, C., Gras, G., Sawaya, BE., Zeichner, SL., Aunis, D., Van Lint, C., and Rohr, O. 2009. p21(WAF1) gene promoter is epigenetically silenced by CTIP2 and SUV39H1. *Oncogene* 28: 3380-3389.

5. Dallos, P., Wu, X., Cheatham, M.A., Gao, J., Zheng, J., Anderson, C.T., Jia, S., Wang, X, Cheng, W.H., Sengupta, S., He, D.Z., and Zuo, J. 2008. Prestin-based outer hair cell motility is necessary for mammalian cochlear amplification, *Neuron* 58: 333-339.

6. Davis, R.R., Newlander, J.K. , Ling, X., Cortopassi, G.A., Krieg, E.F., and Erway, L.C. 2001. Genetic basis for susceptibility to noise-induced hearing loss in mice. *Hear. Res.* 155:

82–90.

7. Di Palma, F., Holme, R.H., Bryda, E.C., Belyantseva, I.A., Pellegrino, R., Kachar, B., Steel, K.P., and Noben-Trauth, K. 2001. Mutations in Cdh23, encoding a new type of cadherin, cause stereocilia disorganization in waltzer, the mouse model for Usher syndrome type 1D. *Nat. Genet.* 27: 103-107.
8. Erway, L.C., Shiau, Y.W., Davis, R.R., and Krieg, E.F. 1996. Genetics of agerelated hearing loss in mice. III. Susceptibility of inbred and F1 hybrid strains to noise-induced hearing loss. *Hear. Res.* 93: 181–187.
9. Golonzhka, O., Liang, X., Messaddeq, N., Bornet, J.M., Campbell, A.L., Mertzger, D., Chambon, P., Ganguli-Indra, G., Leid, M., and Indra, A. 2009b. Dual role of COUP-TF-interacting protein 2 in epidermal homeostasis and permeability barrier formation. *J. Invest. Dermatol.* 129: 1459-1470.
10. Golonzhka, O., Metzger, D., Bornert, J.M., Bay, B.K., Gross, M.K., Kioussi, C., and Leid, M. 2009a. Ctip2/Bcl11b controls ameloblast formation during mammalian odontogenesis. *Proc. Natl. Acad. Sci. U.S.A.* 106: 4278-4283.
11. Gorlin, R.J., Toriello, H.V., Cohen, M.M. 1995. Hereditary Hearing Loss and Its Syndromes. Oxford University Press, New York, Oxford.
12. Grabarczyk, P., Przybylski, G.K., Depke, M., Volker, U., Bahr, J., Assmus, K., Broker, B.M., Walther, R., and Schmidt, C.A. 2007. Inhibition of BCL11B expression leads to apoptosis of malignant but not normal mature T cells. *Oncogene* 26: 3797-3810.
13. Jewett, D.L., Romano, M.N., and Williston, J.S. 1970. Human auditory evoked potentials: possible brain stem components detected on the scalp. *Science* 167: 1517-1518.
14. Johnson, K.R., Erway, L.C., Cook, S.A., Willott, J.F., and Zheng, Q.Y. 1997. A major gene affecting age-related hearing loss in C57BL/6J mice. *Hear. Res.* 114: 83–92.
15. Kamimura, K., Ohi, H., Kubota, T., Okazuka, K., Yoshikai, Y., Wakabayashi, Y., Aoyagi,

Y., Mishima, Y., and Kominami, R. 2007a. Haploinsufficiency of Bcl11b for suppression of lymphomagenesis and thymocyte development. *Biochem Biophys Res Commun.* 355: 538-542.

16. Kamimura, K., Mishima, Y., Obata, M., Endo, T., Aoyagi, Y., and Kominami, R. 2007b. Lack of Bcl11b tumor suppressor results in vulnerability to DNA replication stress and damages. *Oncogene* 26: 5840-5850.
17. Kanzaki, S., Beyer, L.A., Swiderski, D.L., Izumikawa, M., Stöver, T., Kawamoto, K., and Raphael, Y. 1999. Gene disruption of p27Kip1 allows cell proliferation in the postnatal and adult organ of Corti. *Proc. Natl. Acad. Sci. USA.* 96: 4084–4088.
18. Li, H.S., and Hultcrantz, M. 1994. Age-related degeneration of the organ of Corti in two genotypes of mice. ORL J Otorhinolaryngol Relat Spec. 56, 61-67.
19. Morita, Y., Hirokawa, S., Kikkawa, Y., Nomura, T., Yonekawa, H., Shiroishi, T., Takahashi, S., and Kominami, R. 2007. Fine mapping of Ahl3 affecting both age-related and noise-induced hearing loss. *Biochem. Biophys. Res. Commun.* 355: 117–121.
20. Morton, N.E. 1991, Genetic epidemiology of hearing loss. *Ann. N.Y.Acad. Sci.* 630: 16–31.
21. Mulrow, C.D. 1990. Association between hearing impairment and the quality of life of elderly individuals. *J. Am. Geriatr. Soc.* 38: 45–50.
22. Nemoto, M., Morita, Y., Mishima, Y., Takahashi, S., Nomura, T., Ushiki, T., Shiroishi, T., Kikkawa, Y., Yonekawa, H., and Kominami, R. 2004. Ahl3, a third locus on mouse chromosome 17 affecting age-related hearing loss. *Biochem. Biophys. Res. Commun.* 324: 1283–1288.
23. Noben-Trauth, K., Zheng, Q.Y., and Johnson, K.R. 2003. Association of cadherin 23 with polygenic inheritance and genetic modification of sensorineural hearing loss. *Nat. Genet.* 35: 21–23.
24. Ohlemiller, K.K. 2006. Contributions of mouse models to understanding of age- and

noise-related hearing loss. *Brain Res.* 26: 89-102.

25. Siemens, J., Lillo, C., Dumont, R.A., Reymonds, A., Williams, D.S., Gillespie, P.G., and Muller, U. 2004, Cadherin23 is a component of the tip link in hair-cell stereocillia. *Nature* 428: 950–955.

26. Sollner, C., Rauch, G.J., Siemens, J., Geisler, R., Schuster, S.C., Muller, U., and Nicolson, T. 2004. Mutations in cadherin 23 affect tip links in zebrafish sensory hair cells. *Nature* 428: 955–959.

27. Spongr, V.P., Flood, D.G., Frisina, R.D., and Salvi, R.J. 1997. Quantitative measures of hair cell loss in CBA and C57BL/6 mice throughout their life spans. *J Acoust Soc Am.* 101: 3546-53.

28. Topark-Ngarm, A., Golonzhka, O., Peterson, V.J., Barrett, B. Jr., Martinez, B., Crofoot, K., Filtz, T.M., and Leid, M. 2006. CTIP2 associates with the NuRD complex on the promoter of p57KIP2, a newly identified CTIP2 target gene. *J. Biol. Chem.* 281: 32272-32283.

29. Vazquez, A.E., Jimenez, A.M., Martin, G.K., Luebke, A.E., and Lonsbury-Martin, B.L. 2004. Evaluating cochlear function and the effects of noise exposure in the B6.CAST+Ahl mouse with distortion product otoacoustic emissions. *Hear. Res.* 194: 87–96.

30. Wada, T., Wakabayashi, Y., Takahashi, S., Ushiki, T., Kikkawa, Y., Yonekawa, H., and Kominami, R. 2001. A point mutation in a cadherin gene, Cdh23, causes deafness in a novel mutant, Waltzer mouse niigata. *Biochem. Biophys. Res. Commun.* 283: 113–117.

31. Wakabayashi, Y., Watanabe, H., Inoue, J., Takeda, N., Sakata, J., Mishima, Y., Hitomi, J., Yamamoto, T., Utsuyama, M., Niwa, O., Aizawa, S., and Kominami, R. 2003. Bcl11b is required for differentiation and survival of T lymphocytes. *Nat. Immunol.* 5: 533–539.

32. Zheng, Q.Y., Johnson, K.R., and Erway, L.C. 1999. Assessment of hearing in 80 inbred strains of mice by ABR threshold analyses. *Hear Res.* 130: 94–107.

**Fig. 1**. Bcl11b expression and hair cell morphology in *Bcl11b*$^{-/-}$ and *Bcl11b*$^{+/+}$ newborn mice. (A) Immunohistochemistry of Bcl11b in the cochlea. The positions of outer (OHC) and inner (IHC) hair cells are marked. (B) Scanning electron microscopy of outer and inner hair cells in the middle turn of the cochlea.

**Fig. 2**. ABR thresholds of mice of *Bcl11b*$^{+/-}$ and *Bcl11b*$^{+/+}$ genotypes. (A) Data at various frequencies ranging from 8 to 32 kHz are separately shown for C57BL/6 mice at the indicated months of age. (B) Data for BALB/c mice at 9 months of age are shown at different frequency ranges.

**Fig. 3**. The morphology of the middle turn of the cochlea in *Bcl11b*$^{+/-}$ mice and *Bcl11b*$^{+/+}$ mice. (A) Scanning electron microscopy of hair cells in the 6-month old *Bcl11b*$^{+/-}$ mice with hearing loss and control *Bcl11b*$^{+/+}$ mice. Loss of hair cells (indicated by *) and impairment of stereocilia are seen in the left panel, and only impairment of stereocilia in the right upper panel. There are no marked changes in the right lower panel. (B) Hematoxylin staining of spiral ganglia (SGC).

**Fig. 4**. ABR thresholds in mice at the indicated days after noise exposure at 100 dB SPL for 60 min. (A) C57BL/6 mice of *Bcl11b*$^{+/-}$ and *Bcl11b*$^{+/+}$ genotypes. (B) BALB/c mice of *Bcl11b*$^{+/-}$ and *Bcl11b*$^{+/+}$ genotypes.

Fig. 1

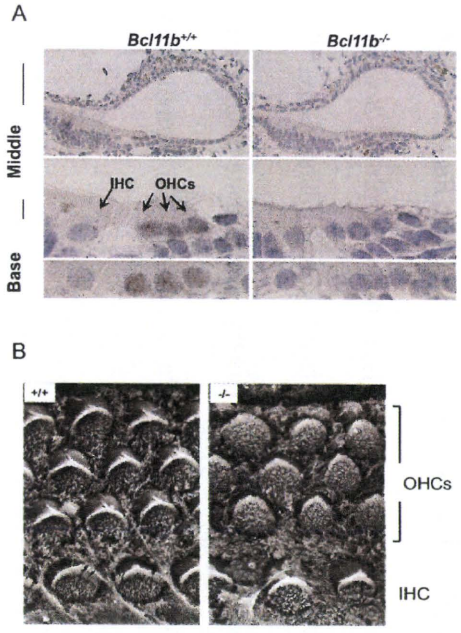


Okumura et al.

Fig. 2

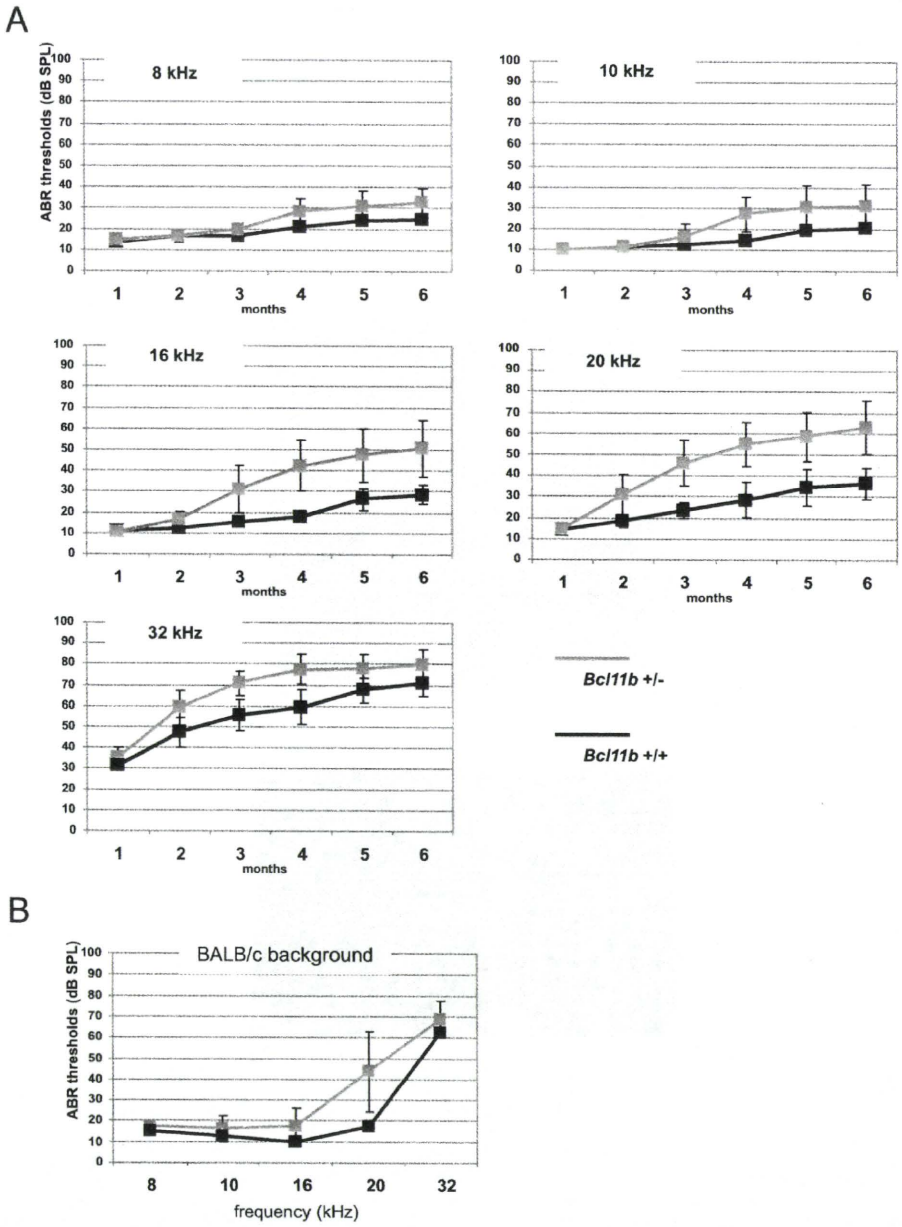


Okumura et al.

Fig. 3

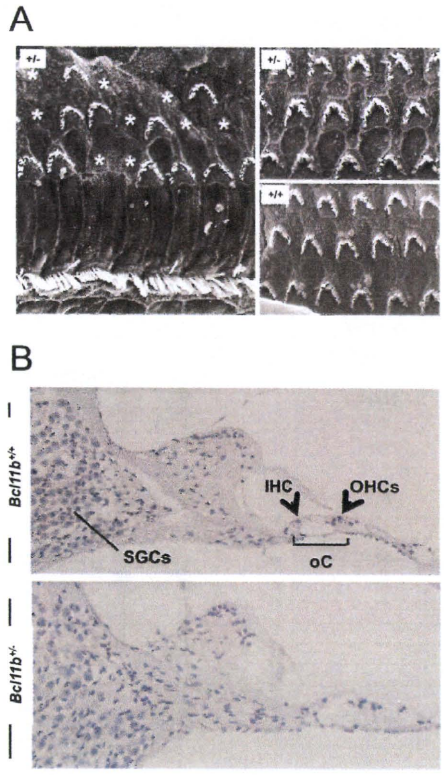


Okumura et al.

Fig. 4

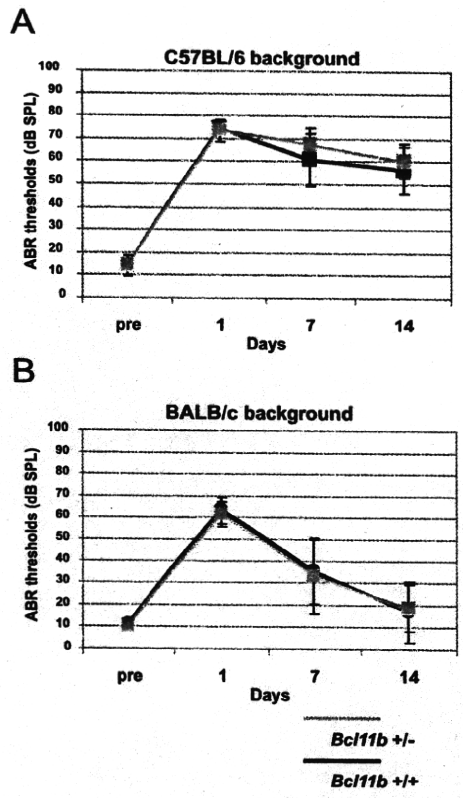


Okumura et al.

MOLECULAR CARCINOGENESIS 49:662–671 (2010)

# Metformin Suppresses Azoxymethane-Induced Colorectal Aberrant Crypt Foci by Activating AMP-Activated Protein Kinase

**Kunihiro Hosono,[1] Hiroki Endo,[1] Hirokazu Takahashi,[1] Michiko Sugiyama,[1] Takashi Uchiyama,[1] Kaori Suzuki,[1] Yuichi Nozaki,[1] Kyoko Yoneda,[1] Koji Fujita,[1] Masato Yoneda,[1] Masahiko Inamori,[1] Akiko Tomatsu,[2] Takeshi Chihara,[2] Kan Shimpo,[2] Hitoshi Nakagama,[3] and Atsushi Nakajima[1]***

[1]*Division of Gastroenterology, Yokohama City University School of Medicine, Yokohama, Japan*
[2]*Division of Biochemistry, Fujita Memorial Nanakuri Institute, Fujita Health University, Mie, Japan*
[3]*Biochemistry Division, National Cancer Center Research Institute, Chuo-ku, Tokyo, Japan*

Metformin is widely used for the treatment of diabetes mellitus. Adenosine monophosphate-activated protein kinase (AMPK) is known to be activated by metformin and to inhibit the mammalian target of rapamycin (mTOR) pathway. The mTOR pathway plays an important role in the protein translational machinery and cell proliferation. We examined the effect of metformin on the suppression of colorectal carcinogenesis in chemical carcinogen-induced models. Seven-wk-old BALB/c mice were intraperitoneally (i.p.) injected with azoxymethane (AOM, 10 mg/kg) and then treated with or without metformin (250 mg/kg/d) for 6 wk (for the investigation of aberrant crypt foci [ACF] formation) or 32 wk (for polyp formation). We next investigated colonic epithelial proliferation using bromodeoxyuridine (BrdU) and the proliferating cell nuclear antigen (PCNA) labeling indices. Furthermore, to examine the indirect effect of metformin, the insulin resistance status and the serum lipid levels were assessed. Treatment with metformin significantly reduced ACF formation. The effect of metformin on colon polyp inhibition was relatively modest. No significant difference in body weight or glucose concentration was observed. The BrdU and PCNA indices decreased in mice treated with metformin. A Western blot analysis revealed that the phosphorylated mTOR, S6 kinase, and S6 protein levels in the colonic mucosa decreased significantly in mice treated with metformin. In conclusion, metformin suppresses colonic epithelial proliferation via the inhibition of the mTOR pathway through the activation of AMPK. As metformin is already used daily as an antidiabetic drug, it might be a safe and promising candidate for the chemoprevention of colorectal cancer. © 2010 Wiley-Liss, Inc.

Key words: metformin; AMPK; chemoprevention; colorectal carcinogenesis; mTOR

## INTRODUCTION

Colorectal cancer (CRC) is the third most common neoplasm in developed countries [1]. Despite major advances in surgical techniques and adjuvant therapy, only a modest improvement in the survival of patients who present with advanced CRC has been achieved. One strategy for diminishing this problem is chemoprevention. Cancer chemoprevention is defined as an intervention using chemical agents that is performed before invasion or to halt or slow the carcinogenic process. Numerous studies have evaluated the possible protective effects of chemopreventive agents, such as supplemental fibers, calcium supplementation, aspirin, nonsteroidal anti-inflammatory drugs (NSAIDs), and selective cyclooxygenase (COX)-2 inhibitors [2]. The most promising agents currently available are COX-2 inhibitors [3], but recent reports have revealed an increased risk of serious cardiovascular events associated with their use [4]. The existence of these side effects led us to search for novel drugs that are both safe and effective. CRC is reportedly associated with lifestyle-related diseases such as diabetes and obesity [5–8], and these conditions might represent new targets for chemoprevention.

Metformin (1,1-dimethylbiguanide hydrochloride) is a biguanide derivative that has been widely used for a long time for the treatment of diabetes mellitus [9]. The molecular mechanism of metformin relies on LKB1-dependent activation of adenosine monophosphate-activated protein kinase (AMPK) [10].

Abbreviations: CRC, colorectal cancer; AMPK, adenosine monophosphate-activated protein kinase; APC, adenomatous polyposis coli; AOM, azoxymethane; ACF, aberrant crypt foci; TBS, Tris-buffered saline; ACs, aberrant crypts; mTOR, mammalian target of rapamycin; S6K, S6 kinase; S6P, S6 protein; BrdU, bromodeoxyuridine; PCNA, proliferating cell nuclear antigen; TUNEL, transferase deoxynucleotidyl uridine end labeling; HOMA-IR, homeostasis model assessment of insulin resistance; HPLC, high-performance liquid chromatography.

*Correspondence to: Division of Gastroenterology, Yokohama City University School of Medicine, 3-9 Fukuura, Kanazawa-ku, Yokohama 236-0004, Japan.

Received 4 June 2009; Revised 19 March 2010; Accepted 19 March 2010

DOI 10.1002/mc.20637

Published online 6 May 2010 in Wiley InterScience (www.interscience.wiley.com)

Interestingly, patients with type 2 diabetes who are prescribed metformin have a lower risk of cancer, compared with patients who do not take metformin [11,12]. These studies suggest that metformin might be a promising candidate for the chemoprevention of CRC, at least in diabetic patients.

Nowadays, several experimental models are available for the study of colon carcinogenesis. Rodent models of colon carcinogenesis can be broadly divided into genetic models (such as $APC^{Min/+}$ mice, a murine model of familial adenomatous polyposis coli [APC]) and chemical carcinogen-induced models (such as azoxymethane [AOM]-induced models). Many chemopreventative studies have been made using a two-animal model of CRC, from which some agents show a consistent preventive effect with both models, but others have given inconsistent, conflicting results [13]. Thus, investigating whether a specific agent inhibits carcinogenesis in different animal models is important.

Previously, Tomimoto et al. [14] showed that metformin suppressed intestinal polyp growth in $APC^{Min/+}$ mice. However, the relationship between the effect of metformin and colon carcinogenesis in an AOM-induced model has not yet been investigated. The objective of this study was to reveal the effect of metformin on the suppression of colon carcinogenesis in an AOM-induced model. We studied the effect of metformin in as short-term study examining the formation of aberrant crypt foci (ACF), which are putative preneoplastic lesions of the colorectum [15,16], as well as its effect on colonic epithelial proliferation. Moreover, a long-term study of AOM-induced carcinogenesis was also conducted.

## MATERIALS AND METHODS

### Chemicals and Animals

AOM was purchased from Sigma (St. Louis, MO). Metformin (Sigma–Aldrich, Inc., St. Louis, MO) was mixed with the powdered basal diet Oriental MF (Oriental yeast Co., Ltd, Tokyo, Japan). The components of this basal diet were as follows: calories, 360 kcal/100 g; protein, 23.6 g/100 g; fat, 5.3 g/100 g; fiber, 2.9 g/100 g; ash, 6.1%; liquids, 7.7%. Food intake was monitored routinely on a daily basis. The mice ate the amount of about 3–4 g of the diets. The mice in the metformin-treated group were fed diets containing 2000 ppm metformin. We used metformin at a dose of about 250 mg/kg/d. The amount of metformin used in this study is higher than that used in diabetic patients (30–50 mg/kg) because previous reports investigating the antidiabetic and antitumor effects of metformin in a mouse model used a higher amount of metformin (250–350 mg/kg) since differences in drug sensitivity are known to exist between rodents and humans [17–19].

Six-wk-old BALB/c female mice were purchased from CLEA Japan (Tokyo, Japan). The mice were treated humanely according to the National Institutes of Health and AERI-BBRI Animal Care and Use Committee guidelines. All the animal experiments were approved by the Animal Care and Use Committee of the Yokohama City University School of Medicine. Four to five mice were housed per metallic cage, with sterilized softwood chips used as a bedding, in a barrier-sustained animal room air-conditioned at 24 ± 2°C and 55% humidity, under a 12-h light: dark cycle. After a 1-wk period of acclimatization to the housing environment and the basal diet, the groups of mice were fed either the basal diet or the experimental diet from 7 wk of age until sacrifice.

### Induction of ACF

To evaluate the effect of metformin on ACF formation, 7-wk-old mice were divided into two groups: mice fed the basal diet as a control group (Figure 1A [Group1]), or mice fed the basal diet plus metformin (Figure 1A [Group2]). Mice were injected intraperitoneally with 10 mg/kg of AOM once a week for 2 wk and sacrificed at 6 wk after the start of AOM injection. The entire colon was removed, gently flushed with Tris-buffered saline (TBS) to remove any fecal contents, opened longitudinally, and fixed flat between filter papers in 10% neutralized formalin overnight at 4°C. After fixation, each colon was rinsed in TBS, stained with 0.2% methylene blue, and stereomicroscopically observed. ACF were identified according to previously described criteria [20,21], and the number of ACF per colon and the number of aberrant crypts (ACs) comprising each ACF were counted.

Moreover, we repeated this study to evaluate the effect of metformin on ACF formation when the metformin was administered after the completion of AOM treatment. The metformin was administered 1 wk after the final AOM injection (Figure 1A [Group3]).

### Induction of Colon Polyps

Seven-wk-old mice were divided into two groups and treated with or without metformin. The mice were injected intraperitoneally with 10 mg/kg of AOM once a week for 6 wk and sacrificed at 32 wk following the initiation of AOM injection (Figure 1B). The colon was removed and fixed in 10% neutralized formalin as described above. The number, size, and locations of the colon polyps were detected macroscopically or stereomicroscopically.

### Western Blot Analysis

The colon was cut open longitudinally and washed with TBS to remove the fecal contents. Then, the colon was laid flat on a glass plate and the distal 2 cm of the colonic mucosa was scraped with a glass slide.

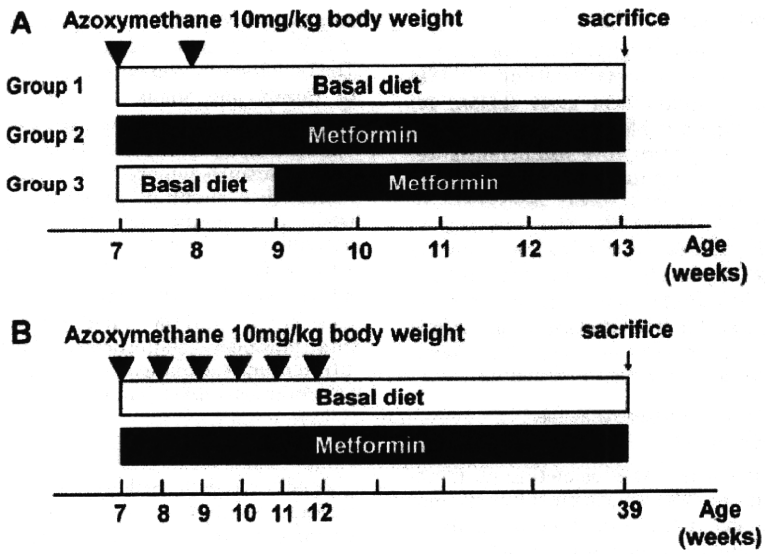


Figure 1. Experimental design for this study. (A) Protocol for AOM-induced ACF. Seven-wk-old mice were treated with or without metformin (250 mg/kg/d). Mice were injected intraperitoneally with 10 mg/kg of AOM once a week for 2 wk and sacrificed at 6 wk after the start of the AOM injections. Group 1: Mice fed the basal diet as a control group. Group 2: Mice fed the basal diet plus metformin after the start of first AOM injection. Group 3: The metformin was administered 1 wk after the final AOM injection. (B) Protocol for the colon polyp study. Seven-wk-old mice were treated with or without metformin (250 mg/kg/d). Mice were injected intraperitoneally with 10 mg/kg of AOM once a week for 6 wk and sacrificed at 32 wk after the start of the AOM injections.

The samples were kept at −80°C until Western blot analysis. The colonic epithelial proteins were extracted using the T-PER tissue protein extraction reagent (Pierce, Rockford, IL) with 1 mM $Na_3VO_4$, 25 mM NaF and one tablet of proteinase inhibitor cocktail (Complete Mini; Roche, Basel, Switzerland). The protein concentrations were determined using the Bio-Rad Protein Assay Reagent (Bio-Rad, Richmond, CA). The extracted protein was separated using sodium dodecylsulfate polyacrylamide gel electrophoresis (SDS-PAGE), and the separated proteins were transferred onto a PVDF membrane (Amersham, London, UK). The membranes were blocked with 5% bovine serum albumin in TBS and probed with primary antibodies specific for AMPK, phospho-AMPK (Thr-172), mammalian target of rapamycin (mTOR), phospho-mTOR (Ser-2448), S6 kinase (S6K), phospho-S6K (Thr-389), S6 protein (S6P), phospho-S6P (Ser-235/236), Akt, phospho-Akt (Ser-473), (all from Cell Signaling Technology, Danvers, MA) and GAPDH (Trevigen, Gaithersburg, MD). Horseradish peroxidase-conjugated secondary antibodies and the ECL detection kit (Amersham) were used for the detection of specific proteins. The results were normalized to the signal generated from GAPDH.

### Cell Proliferation Assay

We evaluated the bromodeoxyuridine (BrdU) and the proliferating cell nuclear antigen (PCNA) labeling indices to determine the proliferative activity of the colon epithelial cells [22–26]. BrdU (BD Biosciences, New Jersey, USA) was diluted in phosphate-buffered saline at 1 mg/mL, and 1 mg of BrdU solution was injected i.p. into each mouse 1 h prior to sacrifice. Twelve mice were tested in each group. Samples embedded in paraffin were sectioned at 4 μm thickness and stained with hematoxylin-eosin or using immunohistochemical techniques. The immunohistochemical detection of BrdU was performed using a commercial kit (BD Biosciences), and a PCNA detection kit (Zymed Laboratories, South San Francisco, CA) was used for PCNA detection. The BrdU and PCNA labeling indices were expressed as the ratio of the number of positively stained nuclei to the total number of nuclei counted in the crypts of the colon. The criteria for selecting the crypts included the presence of a clearly visible and continuous cell column on each side of the crypt. Twenty crypts were randomly evaluated in each mouse.

### Apoptosis Assay

The apoptotic tumor cells were stained using a transferase deoxynucleotidyl uridine end labeling (TUNEL) staining kit according to the manufacturer's instruction (Wako Pure Chemical, Tokyo, Japan). The apoptotic index, which was expressed as the percentage of cells showing positive TUNEL staining relative to the total number of cells in the polyp, was similarly determined. Twelve mice were tested in each group.